THIRD QUARTERLY REPORT

21 February - 20 May 1965

GASEOUS ELECTROLYTES FOR BATTERIES AND FUEL CELLS

by

S. Naiditch, Principal Investigator

Prepared for

NATIONAL AERONAUTICS AND SPACE ADMINISTRATION

CONTRACT NAS 7-326

UNIFIED SCIENCE ASSOCIATES, INC.

826 south arroyo parkway

pasadena, california 91105

murray 1-3486

NOTICE

This report was prepared as an account of Government sponsored work. Neither the United States, nor the National Aeronautics and Space Administration (NASA), nor any person acting on behalf of NASA:

(A) Makes any warranty or representation, expressed or implied, with respect to the accuracy, completeness, or usefulness of the information contained in this report, or that the use of any information, apparatus, method, or process disclosed in this report may not infringe privately owned rights; or

(B) Assumes any liabilities with respect to the use of, or for damages resulting from the use of any information, apparatus, method or process disclosed in this report.

As used above, "person acting on behalf of NASA" includes any employee or contractor of NASA, or employee of such contractor, to the extent that such employee or contractor of NASA, or employee of such contractor prepares, disseminates, or provides access to, any information pursuant to his employment or contract with NASA, or his employment with such contractor.

Requests for copies of this report should be referred to:

National Aeronautics and Space Administration
Office of Scientific and Technical Information
Attention: AFSS-A
Washington, D. C. 20546

THIRD QUARTERLY REPORT

21 February - 20 May 1965

GASEOUS ELECTROLYTES FOR BATTERIES AND FUEL CELLS

by

S. Naiditch, Principal Investigator

Prepared for

NATIONAL AERONAUTICS AND SPACE ADMINISTRATION

CONTRACT NAS 7-326

UNIFIED SCIENCE ASSOCIATES, INC.

826 south arroyo parkway

pasadena, california 91105

murray 1-3486

ABSTRACT

31054

The objective of this program is to investigate the electrochemistry of dense gaseous solutions. Ammonia has been chosen as the solvent because of its low critical temperature and pressure and because it can be studied in glass cells since, unlike water, it does not dissolve glass under supercritical conditions.

Prior to the last quarter, glass cells were developed for the study of dense gaseous electrolytic solutions at pressures of one hundred atmospheres. These cells were constrained from rupturing by use of excess external pressure to compress the glass. In the ensuing experimental studies, two principal difficulties were encountered, mechanical ruptures of the pyrex cells and electrochemical failures; i.e., inception of instability of the emf's or abrupt open circuiting. The latter became especially severe at 90°C, at least 45° below the critical temperatures of the ammoniacal electrolytic solutions.

In the past quarter, causes of the failures were isolated in an extensive series of studies. The cells and operational procedures were then modified to minimize the effects of these causes. It was established that bubbles constitute a principal source of the electrochemical failures. To reduce the tendency to form bubbles, techniques were developed to prepare cells with a low level of volatilizable impurities. The cells and the various chemicals are baked out under vacuum and the chemicals are then transferred into the cell under vacuum conditions. This approach has enabled us to extend the operating temperature of the electrochemical cells to 155°C, where the electrolytic solutions are in the supercritical, dense-gaseous state. The level of traces of water in these cells is very low, lower even than that achievable by ordinary bakeout under vacuum. The only impurities present in appreciable quantities may be sodium amide and hydrogen.

In this series of cells, the remaining problem is that the scatter in the data has been too large. Emf's and conductivities were measured over the whole temperature range. Above room temperature, the emf's increase roughly linearly with temperature, i.e., E/T is approximately temperature independent, in accordance with the expected behavior. The conductivity maximum of the electrolytic solution is a little above room temperature.

In the next quarter, we plan to isolate the causes of the scatter in the experimental data. We shall try to determine whether the scatter in the data is due to bubble formation at the amalgam-electrolytic solution interface.

The mechanical strength of quartz cells will be compared with that of pyrex, to see whether use of quartz is warranted.

Then, we plan to start producing definitive emf, conductivity, and chronopotentiometric data on a series of sodium-amalgam concentration cells over most of the liquid range and into the dense gaseous range of the electrolytic solutions.

1. EXPERIMENTAL TECHNIQUES

In the preceding quarter, two problems interfered with experimental progress; mechanical failures of the glass cells and electrochemical failures. The initial efforts this quarter were on the isolation and removal of these difficulties.

In order to study the problems relating to the mechanical failures of the glass cells, dummy pyrex cells, with no internal glass structures or electrode seals, were made. A number of these dummies, instead of the more expensive complete cells, were tested to destruction. These studies showed that cracking of pyrex cells would occur frequently if filling arms are used since these must be sealed off. The choice thus becomes one of using cells without filling arms or of using quartz (section 1.1).

A series of experiments was carried out to isolate the causes of the electrochemical failure. From these it was found that the principal source of failure was associated with the presence of bubbles. The tendency for formation of these bubbles is probably increased when there are volatilizable impurities or temperature gradients in the cell (section 1.2).

Modifications of the electrical lead through system are described in section 1.3. Also, our revised setup, which enables us to fill more than one cell at a time, is shown in figure 5.

1.1 STUDIES OF CELL MOCKUPS TO REDUCE MECHANICAL FAILURES

In our pyrex cells, mechanical failures have occurred at the seal-off of the side arms used for preparing the amalgam electrodes. In these cells, the seal-off could not be annealed properly without heating the amalgam or the adjacent ring-seals. In the absence of adequate annealing, the glass showed a sharp strain line near the seal-off when examined with polarized light. When mechanical failure occurred, it was generally in this region.

There are two different types of seals used in these cells: (1) the seal-off of the side arms, through which the amalgams and packing were introduced, either in air or in vacuo, and (2) the final seal-off above the freeze cup which severs the cell from the vacuum system. It was noted that the latter seal apparently never failed, whereas almost all failures were at the side arm seals. This was in good part due to the fact that the side arm seals had to be made close to a ring seal and amalgam and therefore the annealing in this region could not be done as thoroughly as needed.

In order to obtain more data on this problem, dummy pyrex cells were made and their mechanical behavior evaluated in the bomb at elevated temperatures under external pressure. In these studies, the glass continued to crack near the seal-off of the side arms. With the particular design in use at the beginning of the quarter (figure 1), it was not possible to anneal the seals adequately without overheating the neighboring regions.

We tried a number of packings, such as wet asbestos, to protect the glass in the region of seal-off, hoping thereby to be able to anneal more thoroughly. We did not obtain satisfactory results. The

failure pressures for tests with six mockups of the cells in use at the end of the preceding quarter are shown in table 1.

Next (figure 2), we moved the seal-off region away from the amalgam and ring seal region. This helped because it gave us more room in which to flame anneal. However, it caused trouble because of our limited geometry inside the bomb. This reduced the sharp strain line at the seal-off, which had been the major source of failure. The results for two mockup cells are given in table 2. There was a tendency of these cells not to fit in the bomb.

We then tried a third type of cell (figure 3). The idea here was to simulate the conditions under which the cell to vacuum system severance seal-off was made, since this is the seal-off that doesn't fail. Here we connected a tube to the bottom of each electrode compartment and passed each of these four tubes to the region below the cell. The space was arranged so that there would be room for annealing in the region of each seal-off. However, the long arms themselves were weak, so that this approach was not satisfactory. The results of tests for three mockups of this type of cell are shown in table 3.

We would like to be able to subject the cells to compressive pressure differentials of 150 atms, since this would simplify experimental procedures in the actual tests. The pressures at which failures occur have been irreproducible; this is in part attributable to the nature of glass.

As a consequence of these studies, we have redesigned our preparation system so that we are now using cells without any side

arms. In the near future, we plan to build and test quartz cells, since it is generally not necessary to anneal quartz.

1.2 ELECTROCHEMICAL FAILURES OF THE CELL

Our most disturbing problem has been that the emf's of our cells frequently become unstable or the cells open circuit. In particular, these malfunctionings have occurred occasionally when the heater is turned on and regularly when the temperature rises to 90°C. We have considered the following as possible sources of these electrochemical failures.

1. Exposure of the tungsten leads to the electrolytic solution above the amalgam.

2. The breaking apart of the amalgam-insoluble salt interface.

3. Formation of an insulating crust on the surface of the amalgam by insoluble contaminants.

4. Formation of bubbles on the surface of the amalgam and in the solution itself.

It will be seen in the following section that the principal source of failure is that of bubble formation, and that this is undoubtedly aggravated by the presence of (volatilizable) impurities.

1.2.1 Tungsten Lead Problems

We have found that when the tungsten leads, whether platinized or not, are in direct contact with the electrolytic solution,

i.e., are not completely immersed below the surface of the amalgam (correct positioning is shown in figure 6), the cells recover slowly after current is drawn from them. We also have the impression that there is a small amount of instability of the emf's associated with such exposure. In contrast, when platinum electrodes are used in aqueous solution, contact of the platinum with the electrolytic solution generally does not produce such effects. In our case, if the hydrogen over-voltage on tungsten or platinized tungsten is low in liquid ammonia, then the following may take place at the single electrode:

Amalgam:

$$Na = Na^{+} + e^{-}$$

Exposed Tungsten:

$$NH_3 + e^{-} = NH_2^{-} + 1/2\ H_2$$

The overall parasitic reaction at this junction is then

$$Na\ (amalgam) + NH_3(NH_3) = NaNH_2(NH_3) + 1/2\ H_2(W).$$

Fluctuations in emf may take place as hydrogen bubbles break away from the tungsten surface, exposing the surface to renewed electrochemical action. When freshly cleaned tungsten electrodes, completely immersed in the amalgam, have been used, the emf's have been irregular. Platinizing of the electrodes improves the stability. We have measured the electrical resistance of tungsten, with and without platinization, to mercury (or amalgam) and have found the resistance to be negligible in both cases. The origin of this difference in behavior between tungsten and platinized tungsten surfaces completely immersed in the amalgam is not clear to us.

In our earlier studies we lost a few cells when the welds (which can be seen in figure 6) between the stranded nickel wires and the tungsten lead-throughs opened up. The tungsten leads in those cells were 0.030" in diameter. To eliminate this breakage, we modified our cells so that we could use heavier tungsten leads of 0.080" diameter. Since that time, there have been no failures from snapping off the leads. Introduction of the heavier leads has given rise to two problems. It is more difficult for the glass blower to place the exposed ends of the heavier tungsten so that they will be below the surface of the amalgam, and the heavier leads probably aggravate the tendency for bubble formation.

In connection with the former, namely, the location of the exposed part of the tungsten lead, we think that this factor may be responsible for some of the scatter in our data in our current series of measurements. When we ran the experiments, we were primarily concerned with eliminating the open circuiting, and did not concern ourselves with the more minor problems which will now be attacked.

One way of resolving the problem would be to use more amalgam to cover the ends of the electrodes. Unfortunately, we have found that when we use large amounts of amalgam, the glass sometimes cracks during the freezing or thawing of the amalgam. Hence we plan to modify the glass structure to accommodate the electrode.

In the cells now being fabricated, we plan to evaluate the difference between platinum and tungsten as follows: The end of the tungsten will be welded to a short length of fine platinum wire. The nonex glass bead will cover the tungsten and continue to the

end of the platinum. In this way only the end of a fine platinum wire is exposed. Results with this will be compared with those obtained with tungsten and platinized tungsten leads.

As mentioned above, the heavier leads may aggravate the tendency for bubble formation. The leads are welded to heavy stranded nickel wire on the outside and dip into amalgam on the inside. The outside wire is closer to the heat source than the glass, and also is a better heat conductor. When we raise the temperature, the heat will be transmitted into the amalgam relatively faster than through the glass into the solution. Hence, there is a tendency for the amalgam at the ammonia interface to be hotter than the bulk of the ammoniacal solution and therefore to produce bubbles.

1.2.2 The Amalgam-Insoluble Salt Interface

The electrodes used at the beginning of the quarter consisted of an amalgam with finely ground insoluble salts on their surfaces or a paste of the amalgam and salt. As the temperature was raised, these cells invariably failed at or below 90°C, either becoming very unstable or open circuiting. The original emf was recovered within a day or two after the temperature of the cells was lowered.

One possible source of these instabilities was that the amalgam-insoluble salt interface was breaking apart. As the critical temperature of the electrolytic solution is approached, the liquid may become very turbulent if there are even small temperature gradients in the cell. Such vigorous turbulence could blow the insoluble salt off the surface of the amalgam. In some experiments

we packed glass wool tightly above the salts, in others we used no glass wool. We found no marked difference between these two sets of conditions.

More than one electrode has often failed simultaneously. It is unlikely that the cause of simultaneous failures can be the formation of oxide crusts on amalgam surfaces or the breaking apart of the junction between amalgam and insoluble salt. As an example, in one cell with three "good" and one open electrode, the three good electrodes failed simultaneously almost immediately after the heat was turned on to raise the temperature inside the bomb. The reason it took place simultaneously at this time may be because when heating current is turned on the metal leads pick up heat rapidly and transmit it to the electrode. This overheating at the electrode-solution interface may tend to produce bubbles.

We next prepared an amalgam concentration cell which uses only soluble salts, to see whether the instabilities persisted in the absence of an insoluble salt-amalgam interface.

With our first sodium amalgam concentration cell (No. 49) which used soluble sodium iodide, we found we still got the same characteristic instabilities. This cell had cracked during preparation and had been resealed and rebaked. Hence, there must have been a fair amount of oxides present so that the cell was contaminated. Since we observed the same problems with this cell as in ones using insoluble salts, the basic difficulties we have encountered are probably not due to break apart of the amalgam-insoluble salt interface, but to either formation of an insoluble insulating crust on the surface of the amalgam or to bubbles. Therefore,

we feel that at a later stage we can go back to the original electrochemical cells if we vary the method of preparation appropriately.

The behavior of cell No. 49 will now be discussed in more detail. On turning on the heaters, the cells open circuited. The bomb was cooled and opened. We observed bubbles visually. The bubbles disappeared on standing, and the cell became functional again. The erratic behavior of this cell is shown by the emf between the top and bottom electrodes. The day after the cell had been prepared, the emf at room temperature was 168.8 millivolts, the emf being steady within $\pm$ 0.2 millivolts over a period of 45 minutes. After turning on the heaters, the values of the emf's fluctuated between 40 and 670 millivolts. At this time the bomb was opened and bubbles were observed visually in the connecting arms. After the bubbles were eliminated, the emf returned to 170 millivolts.

1.2.3 Insulating Crusts, Contaminants and Bubbles

At this stage we had fairly convincingly pinned down the principal difficulty as being due to the presence of contaminants or to bubbles. Therefore, for the next experiments, whose data will be discussed in section 2, we set up a sodium amalgam concentration cell without side arms, in which the cell itself was baked under vacuum. Triply distilled mercury was placed in the cell. Then the cell was sealed onto the system. The cell with mercury, the soluble salt in a separate chamber above the cell, and triply distilled sodium encapsulated with a break seal, were all baked out at 400°C under vacuum, and all except the sodium were pumped continuously. After cooling, prepurified ammonia was condensed

into the storage vessel containing metallic sodium for further drying (figure 5). Then the break seal was opened and the sodium distilled onto the walls. Ammonia was then condensed in the freeze cups, dissolving the sodium and the salt, and run into the cell. Then with the cell at dry ice-alcohol temperatures, liquid nitrogen was poured into the freeze cup, the system above the freeze cup evacuated, and the cell sealed off. It took about a day at $0^{\circ}C$ for the color of sodium in solution in the ammonia to disappear. Some sodium dissolved in the mercury to form an amalgam, as evidenced by the emf of the electrodes and by chemical analyses of the amalgams.

Some of the sodium may also have reacted with the ammonia to form sodium amide plus hydrogen. In a future run, we plan to leave the cell connected to the vacuum system until all the sodium disappears, then pump off the hydrogen before seal-off, since hydrogen might be a nucleating agent for the bubbles.

These new cells are undoubtedly the dryest electrochemical cells ever prepared. Not only have the glass and various chemicals been baked out under vacuum, but after the cell has been prepared, most of the walls have been exposed to a sodium-ammonia solution for a day. The sodium-ammonia solution is effective in removing traces of sorbed water left on glass surfaces during bakeout under vacuum.

With these new cells, in which the level of contamination is extremely low, the only major impurities present are sodium amide and hydrogen. If the sodium amide concentration is low, so that it remains in solution, it will not affect the behavior of the

cell. Using these cells, we have successfully extended the measurements of emf and conductivity to 155°C. Instabilities remain in the data. We think there may be two sources for these instabilities which are probably removable, and a third that may not be removable. (1) The exposure of the tungsten electrodes to the solution may lead to instabilities, and will be eliminated in our next runs. (2) Possibly the principal source of instability is the presence of hydrogen produced by the reaction between the dissolved sodium and ammonia in the first day. This will be removed in our next runs. (3) If hydrogen is being produced throughout the run by the nonelectrochemical side reaction of sodium amalgam with ammonia, this source of contaminants is not removable, except by changing the electrode system itself, or the solvent.

We interpret the source of our difficulties as follows: bubbles are being formed in our solutions because of a number of circumstances that usually do not bother the electrochemist. (1) We are operating under the vapor pressure of solvent, so that we do not have a gas at atmospheric pressure reducing the tendency of bubble formation. (2) Our leads, and therefore our amalgams, are warming up faster than the electrolytic solution so that at the interface between amalgam and solution the vapor pressure of ammonia is higher than in the bulk of the solution. The tendency to form bubbles may be greater at a foreign surface than in a homogeneous medium. (3) If hydrogen is present, it may help form bubbles by acting as a nucleating agent for the bubbles.

There is a vast amount of pertinent literature on the subject of bubble formation. For example, in distillation, the following related phenomena have been observed. "When a liquid is boiling

in a vessel, bubbles of vapour are evolved at definite points where small air bubbles, either evolved on first heating the liquid or adhering to the surface of the vessel, are present. As boiling proceeds, these points decrease in number and finally disappear. The temperature then rises by several degress (13.8° with water) without boiling taking place, until finally a rush of vapour occurs, usually in one large bubble from the bottom of the vessel, the temperature sinking to the boiling-point." (Partington, Advanced Treatise on Physical Chemistry, Vol. II, Wiley, 1951, p. 278.)

Our success in the past quarter in extending the working range of our cells by 65°C is undoubtedly related to the improved cleanness of our system in that we have fewer nucleating agents and therefore less tendency for bubble formation. It should be possible to overheat part of the cell locally by a few degrees without bubble formation if the system is sufficiently free of contaminants. This may be seen from the following quotation. "Similarly, in a pure liquid such n-pentane, superheating at 1 atm. pressure from the equilibrium boiling point (36°C) to about 120°C is possible if the liquid is highly purified. Conversely, one may raise the pressure over n-pentane and heat the liquid to any desired temperature above the normal boiling point, and then suddenly reduce the pressure back to 1 atm. The time interval that elapses before boiling occurs is related to the probability of spontaneous nucleation at the temperature concerned." (Davies and Rideal, Interfacial Phenomena, 2nd Ed. 1963, Academic Press., p. 394.) REF.

In these experiments with highly purified systems, instabilities have remained. These may not be attributed to insoluble insulating

crusts on the amalgams -- there just isn't enough foreign material (including sodium amide) to form such crusts. Hence, we must conclude that the principal problem is that of the presence of bubbles, and that the tendency to form bubbles is increased by impurities.

Our conclusion as to the principal source of the open circuiting difficulty, namely, bubbles, also answers the question as to why Yost and co-workers didn't report such difficulties. Since their cells were under an atmosphere of hydrogen, their conditions were less conducive to bubble formation than ours, which are under only the vapor pressures of the solutions.

We think that the bubbles may be forming at the amalgam-solution interface. They probably need a nucleus or catalyst for their formation. Also, there may be a slight excess vapor pressure existing near the amalgam since the largest temperature gradient in the system is probably at the amalgam-solution interface. Traces of hydrogen may be produced at the amalgam surface by the non-electrochemical reaction between the sodium-amalgam and ammonia. If the rate of this reaction is small, then we may be able to obtain a stable cell. Based on our experience, we think that this is possible.

We have found that when we place a load on some of the half cells the stability of all the cells seems to decrease. In our cells, because of the method of preparation at the moment, the principal impurity is sodium amide and hydrogen. Even if we bypass the formation of hydrogen during the preparation of the cell, we will

be producing it when we put power through the cell or withdraw power from the cell.

In conclusion, we have definitely established that even with highly purified cells, electrochemical failures can occur. Since we have excluded insoluble salt interfaces and insoluble crusts, the only probable source of such failures is clearly bubble formation.

1.3 BOMB HEAD

The leads, which passed through a head from the inside to the outside of the bomb, originally consisted of coaxial wires fabricated to our specifications by a thermocouple manufacturing company. The inside wires (0.015 inches in diameter) were so fine that they broke frequently. Another difficulty was that when a sample would rupture in the bomb, the ceramic insulation would saturate with ammonia. When this happened, the insulation resistance of the wire to ground could be reduced from 20 megohms to less than 8000 ohms. Then, the whole head had to be disassembled and new wires inserted through a five-wire conax fitting.

A new head has been designed and built to provide a more satisfactory system. It contains one thermocouple and four teflon coated copper wires of 0.062 inch diameter, each sealed with its own separate pressure fitting. Thus any wire can be replaced without disturbing the seals on the other wires. Wires are replaced when their resistance to ground drops below 20 megohms. Since the diameters of the wires are now larger, they are much easier to work with than those in the previous model. The space between the teflon sleeving and the stranded wire is filled with a silicon

rubber compound under pressure so that there is a negligible pressure leak rate even at a pressure differential of 200 atms. With teflon sleeving, there is no danger of the insulating material becoming conductive when exposed to ammonia.

2. EXPERIMENTAL STUDIES

Our present techniques, which are based on the results of the preceding studies, have enabled us to extend the operating range of the electrochemical cells by 65°C, into the supercritical, dense-gaseous region of the electrolytic solutions.

2.1 BAKEABLE ELECTROCHEMICAL CELLS

We are currently using a technique in which the cells and the chemical components are baked out under vacuum and then handled in vacuo in order to maintain a state of high purity and a minimum level of volatilizable contaminants. The first bakeable cell to be prepared and filled (figure 3) was cumbersome and fragile. It was so designed that, after bake out under vacuum, triply-distilled mercury could be distilled into each of the four electrode compartments through separate filling arms, then triply-distilled sodium introduced similarly by distillation into the same filling arms.

In contrast to the complexity of this first cell, we are now using a cell without any side arms (figure 4). Our present cell is a sodium amalgam concentration cell in which each amalgam has a different concentration of sodium. The electrolytic solution is sodium iodide in ammonia. In this cell the mercury is introduced in air before the cell is sealed onto the vacuum system. After sealing on the cell and evacuation, the cell, mercury and salt are baked out under vacuum. The sodium is hermetically sealed in a capsule with break seal during bake-out. On cooling, the sodium is distilled into the system. The salt and sodium are then moved by washing them into the cell with liquid ammonia. After this, the amalgams are formed by dissolution of the metallic sodium which is in solution in liquid ammonia. The preparation system is shown in figure 5.

2.2 EXPERIMENTAL DATA FOR SODIUM AMALGAM CONCENTRATION CELLS

2.2.1 Cell No. 49

Cell No. 49 (figure 3) was the first sodium concentration cell prepared. This cell design has since been abandoned because of its fragility and complexity of handling. Triply distilled mercury and triply distilled sodium were distilled separately into each electrode compartment. The cell was accidentally broken during the next operation in which the cell is filled with ammonia. The ammonia was allowed to evaporate slowly. Then the cell was repaired with a minimum of glass blowing and sealed back onto the vacuum system. The cell was evacuated, baked at 120°C for half an hour, allowed to cool, then refilled with ammonia, and sealed off. Subsequent emf measurements were erratic, possibly due to oxidation of sodium when the contents of the cell were exposed to the atmosphere. Bubbling at the electrodes was particularly severe. The values of the emf as a function of temperature are given in table 4. These data show the erratic behavior in a contaminated cell. It is clear from these data that electrochemical failures can occur in the absence of insoluble salts. The poor behavior of this cell indicates that contamination may be an important factor in such failures.

2.2.2 Cell No. 50

All cells after No. 49 are being made without filling arms (figure 4). The mercury is poured into position prior to sealing the cell onto the system. After bake-out the sodium is distilled, then it and the salt are dissolved in liquid ammonia, and the resulting solution allowed to flow down the capillary into the cell. This filling technique leads to similar concentrations of sodium in the four electrode compartments, thus the emf's generated are small.

With the earlier procedure of distilling in the sodium (cell 49), emf's of 0.5 volts were obtained whereas with the present procedure, emf's range from 0.01 to 0.2 volts.

Cell No. 50 broke in the bomb prior to measurement but gave fairly stable readings until the evaporation of the ammonia proceeded too far. Measurements were made only below room temperature. The source of rupture is probably a new one which arises as follows: sodium is introduced in solution in ammonia. Then the cell is sealed off. It takes about a day at $0^{\circ}C$ before all the blue color disappears. During this time, some of the sodium dissolves in the mercury, forming the desired amalgam. In addition, the foreign material, mercury or amalgam, may catalyze the reaction of some of the sodium with ammonia,

$$Na + NH_3 = NaNH_2 + 1/2\ H_2,$$

which produces a gas, hydrogen. If this reaction takes place to a sufficient extent, it may build up sufficient pressure to crack the cell.

The emf's (table 5) are plotted as a function of temperature in figure 7. In contrast to the curves for the other samples, the slope of the curve is negative. This may be due to a phase separation in one of the amalgams. The overall cell reaction is

$$Na\ (X_2'\ \text{in Hg}) = Na\ (X_2''\ \text{in Hg})$$

where $(X_2'\ \text{in Hg})$ designates the mole fraction of sodium in the primed amalgam.

As long as no current is drawn, then, the emf is independent of the conductivity of the electrolytic solution, and therefore of the concentration of sodium iodide. This condition prevails until so much ammonia evaporates that the electrolytic solution resistance becomes comparable with the input impedance of the potentiometer. Then the emf will start dropping. Decreasing emf's were observed as the cell started to fail.

The function, E/T (i.e., emf/temperature) should be approximately temperature independent over the limited temperature range of this experiment. Instead, it is decreasing with increasing temperature. Hence some other process is occurring. One such process may be a phase separation in one of the amalgams. Then, instead of the above process, the following may be occurring. The fugacity or activity of sodium in the more concentrated amalgam will be a function of temperature determined by the phase diagram. The activity of sodium in the other amalgam is almost temperature independent.

$$a_2'' = \gamma_2'' X_2''$$

where a_2'' is the activity, γ_2'' the activity coefficient and X_2'' is the mole fraction. γ_2'' will vary slightly with temperature whereas X_2'' is temperature independent.

In contrast, in the case of the phase separation, the composition of each of the phases, X_2', varies with temperature. This may introduce a ΔH term of opposite sign into the process.

2.2.3 Cell No. 51

The next cell, No. 51 (table 6), gave stable emf readings from -30 to +20°C (figure 8). Emf's and conductivities were then measured

alternately from -40°C to +136°C, the critical region of the electrolytic solution. These emf's were less stable and reproducible than the first emf's in which no currents were passed through the cell. The emf's (figure 9), increase approximately linearly with temperature. The ratios of emf's to temperatures (figure 10), scatter too much to ascertain any temperature dependence.

The specific conductivity versus temperature (figure 11) is roughly parabolic. The conductivity maximum occurs at a temperature of about 40°C.

When lowering the temperature rapidly there was a break in the data that persisted for quite a time. These data are indicated by "X" and "*". The data in the tables are recorded sequentially in time so that when a bubble forms its effect can be seen on the subsequent consecutive measurements. In this case the postulated bubble can be seen in the data as follows: Examination of the curve shows that the emf's have dropped and are recovering slowly. Simultaneously the resistance of the cell has increased, i.e., the conductivity has decreased. It will be noted that it takes longer for the conductivity to recover than for the emf. This is not unreasonable since the emf measuring instruments can give correct readings if a series resistance is introduced; whereas, this series resistance will show up in the conductivity measurements.

Above about 125°C the behavior of the conductivities appears to change abruptly. This is in fairly good accord with the usual behavior where the conductivities become almost temperature independent when the cell is filled completely with a single fluid. Under this condition, i.e., change in temperature at constant volume, the density is constant.

The sample ruptured a few degrees above the critical point of pure ammonia because the initial fractional filling of the cell was too great. As a consequence, calibrated fiducial marks are now being placed on the cells to guide the initial filling.

2.2.3.1 Chemical Composition of the Amalgams in Cell No. 51

The amalgams of the two emf measuring electrodes were analyzed. The amalgam in the upper electrode was largely lost when the cell ruptured. The analysis of the amalgam in the lower electrode was as follows:

Total weight of amalgam	9.4889 g
Sodium	0.00030 g
Mercury	9.4886 g
Mole fraction of sodium	0.00027

The chemical analysis was carried out as follows. The amalgam was placed in an Erlenmeyer flask with 1.0 ml 0.1268 N HCl and 25 ml of water and stirred with a teflon-clad magnetic bar for several hours. Back titration using phenophthalein indicator required 1.12 ml 0.1017 N KOH solution, or 0.0129 mmoles of base, i.e., Na from the amalgam.

From the emf data, the concentration of the upper electrode may be established as follows: For a concentration cell,

$$ENF = - RT \ln (a_2'' / a_2').$$

Assuming that the activity coefficients of sodium in the two amalgams are equal, the mole fraction of sodium in the upper emf amalgam is 0.00044.

2.3 SUMMARY

Although the initial data are rough, several tentative conclusions can be drawn. Before detailed examination conclusions can be made; however, we must obtain more refined data. The stability of the cells generally has improved considerably over those of the preceding quarter. When we passed current through the cells, the stabilities became poorer, and the data became more irregular.

Insofar as the emf's are concerned, these behave approximately satisfactorily. The ratio of emf to absolute temperature should be almost temperature independent, which it is. In contrast, the specific conductivities of the solution vary strongly with temperature. The general shape of the conductivity-temperature curve is similar to those in the literature.

Because of instrumental interactions, we have ordered an electronic potentiometer Calibrations Standards, Model DC 110B (Company provided). This instrument has an input impedance at null of 1000 megohms. It will be used for measuring emf's across the two reference (emf) electrodes.

The recorder we have been using is a Bausch and Lomb VOM 5. It has an input impedance of 10 megohms and requires a source of less than 150 kilo-ohms. We have observed that there appears to be a cross coupling between this and an electronic potentiometer across the reference electrodes. This will be checked when the new potentiometer is delivered around July 28. In the meantime, we have used a similar instrument of slightly lesser accuracy, the Calibration Standards Model DC 100B.

If the impedance of the recorder is too low for our system, or if cross-coupling continues, there are two things we can do. We can

buy a battery pack for the electronic potentiometer to reduce ground loops, or we can place a DC vacuum tube voltmeter into the circuit, and connect the recorder to an output plug on this instrument.

So far there has been no new type of electrochemical behavior in our system. When a gaseous electrolyte has been used, the equilibrium emf's for an amalgam concentration cell have been approximately those expected thermodynamically. Hence, chronopotentiometric data will be used to find differences in behavior between the liquid and gaseous electrolytic states.

3. PLANS FOR NEXT QUARTER

The mechanical strength of quartz cells will be evaluated and compared with that of pyrex. The scatter in the data has been large; therefore, we will examine the sources of the scatter to isolate and reduce them. We are also modifying our instrumental setup to reduce the cross-coupling of the various instruments. Then we expect to start producing definitive data of emf's and conductivities as well as chronopotentiometric data on sodium amalgam concentration cells. Chronopotentiometry will be used as a tool to examine differences in the behavior of the electrochemical processes at amalgam-liquid and amalgam-dense gaseous electrolytic solution interfaces.

4. ERRATUM

Substitute uranium glass (Corning 3321) for nonex glass throughout this report.

TABLE 1. FAILURE PRESSURES FOR MOCK-UPS SHOWN IN FIGURE 1

Sample	Protection of Adjacent Region During Seal-off of Side Arms	Failure Pressure
1s	Aluminum Foil	<240 atms
2s	Wet Asbestos	290
3s	Wet Asbestos	150
4s	Wet Asbestos	(340) 258*
6s	Aluminum Foil and Wet Asbestos	(340) 40*
8s	None	80

*Noise from bomb (associated with failure) heard during release of pressure after reaching 340 atms.

TABLE 2. FAILURE PRESSURES FOR MOCK-UPS SHOWN IN FIGURE 2

Sample	Failure Pressure
1t	<310
2t	170-340

TABLE 3. FAILURE PRESSURES FOR MOCK-UPS SHOWN IN FIGURE 3

Sample	Failure Pressure
1r	30
2r	(150) 60*
3r	<340

*Went up to 150 atms. Sample broke on releasing pressure.

TABLE 4. DATA FOR CELL NO. 49

TEMPERATURE °C	EMF VOLTS	REMARKS
-36.3	0.0530	
-21.9	0.0442	
- - - - - - - - - - - -		Passed current, erratic readings. Bubble observed.
-34.1	0.680	
- - - - - - - - - - - -		Passed current, again unstable.
-13.5	0.302	
- 8.5	0.3601	
+74.3	0.170	Took up to temperature to stabilize.
Next Day		
22.0	0.1279	
- - - - - - - - - - - -		Passed current, erratic.
22.0	0.410	
22.0	-0.07	Erratic.
40.3	0.4725	
65.2	0.345	
- - - - - - - - - - - -		Passed current, then allowed to stabilize.
56.5	0.450	
56.5	0.2570	
58.2	0.449	
85 to 77	0.820	
80	0.230	
68	0.8312	

TABLE 5. DATA FOR CELL NO. 50

TEMPERATURE	EMF, VOLTS	REMARKS
- - - - - - - - - - - - -		Cell broke in the bomb
19.9	0.01685	
20.5	0.01850*	Current passed through working electrode
20.7	0.01685	
-28.0	0.02580	
-13.9	0.02004	
- 7.4	0.01853	
- 1.8	0.01786	
+ 1.8	0.01514*	Current drawn from reference electrodes
+ 8.2	0.01775	
+11.1	0.01726≠	
+14.0	0.01575*	
+16.9	0.0107 *	Current passed through working electrodes
+18.1	-0.0820 *	
+18.2	0.0110 *	
+18.2	-0.08 *	
+24.8	-0.07 *	

*Points not plotted

≠After this (the data are sequential in time), the emf's decreased in magnitude, then open circuited. This behavior is compatible with increased resistance, then open-circuiting due to evaporation of ammonia.

TABLE 6 - CELL NO. 51

TEMPERATURE, °C	EMF, VOLTS	CONDUCTIVITY, (OHM CM)$^{-1}$	E/T, MICROVOLTS/°K	
-25.6	.01171	No Conductivity Measurements	47.3	
-29.3	.01112		45.6	
-29.1	.01093		44.8	
-24.2	.01084		43.5	
-23.0	.01092		43.6	
-19.3	.01120		44.1	
-17.2	.01150		44.9	
-15.9	.01161		45.1	
-12.5	.01194		45.8	
-10.3	.01194		45.4	
- 7.1	.01211		45.5	
- 4.9	.01210		45.1	
- 2.5	.01214		44.8	
- 0.6	.01216		44.6	
+ 9.0	.01222		43.3	
+ 9.3	.01224		43.3	
+11.3	.01248		43.9	
+17.6	.01281		44.0	
-15.2	.01125		43.6	Very rapid cooling.
-41.2	.00703[X]		30.3[X]	
-39.5	.00613[X]		26.2[X]	
-40.8	.00595[X]		25.6[X]	
-47.0	.00616[X]		27.2[X]	

[X] Data plotted as "X" on graphs

TABLE 6 - CELL NO. 51

TEMPERATURE, °C	EMF VOLTS	CONDUCTIVITY, (OHM CM)$^{-1}$	E/T, MICROVOLTS/°K
-48.2	.00702*	4.50* x 10^{-3}	31.2*
-46.5	.007441*	4.40*	32.8*
-42.0		4.38*	
-38.0	.00883*		37.5*
-37.0		4.41*	
-34.8		4.35*	
-33.2	.00939*		39.1*
-32.0		4.40*	
-31.1	.00943*		39.0*
-29.8		4.47*	
-27.0	.01042		42.3
-26.8		4.49*	
-24.6	.01100		44.3
-23.1		4.54*	
-21.7	.01122		44.6
-20.6		4.61*	
-19.6	.01109		43.7
-18.3		4.68*	
-17.0	.01127		44.0
-15.9		4.92*	
-15.1	.01122		43.5
-14.2		5.00*	
-36.7	.01076		45.5

Data plotted as "" on graphs

TABLE 6 - CELL NO. 51

TEMPERATURE, °C	EMF, VOLTS	CONDUCTIVITY, (OHM CM)$^{-1}$	E/T MICROVOLTS/°K
-35.8		5.03×10^{-3}	
-28.3	.01026		41.9
-26.3		5.02	
-25.2	.01053		42.5
-23.9	.01048		42.0
-23.2		5.01	
-21.9	.01018		40.5
-19.9	.01026		40.5
-19.0		5.10	
-18.5	.01035		40.6
-18.1		5.14	
-16.9	.01046		40.8
-16.3		5.16	
-15.3	.01056		41.0
-13.3	.01070		41.2
-12.4		5.22	
-11.6	.01107		42.3
-10.9		5.29	
-10.5	.01084		41.3
-10.0	.01086		41.3
- 8.7	.0109	5.43	41.2
- 7.6	.01105		41.6
- 5.2	.01115		41.6
+10.0	.01153		40.7
12.0		5.91	
13.2	.01172		40.9
13.2	.01183		41.3
16.0		5.99	

TABLE 6 - CELL NO. 51

TEMPERATURE °C	EMF, VOLTS	CONDUCTIVITY (OHM CM)$^{-1}$	E/T, MICROVOLTS/°K
16.9	.01191		41.1
17.5	.01207		41.5
19.0		6.03×10^{-3}	
19.9	.01215		41.5
23.3	.01245		42.0
36.1		6.13	
39.8	.01333		42.6
45.2	.01400	6.24	44.0
49.0	.01429		44.4
50.0		6.09	
50.7	.01424		44.0
53.4	.01401		42.9
56.2	.013815		41.9
58.3		5.81	
59.5	.01324		40.0
60.3		5.70	
61.8	.01315		39.3
61.8	.01354		40.4
62.5	.01342		40.0
65.0		5.54	
65.9	.01321		39.0
66.9		5.41	
70.3	.01311		38.2
73.6		5.19	
74.4	.01306		37.6
75.4	.01318		37.8

TABLE 6 - CELL NO. 51

TEMPERATURE °C	EMF, VOLTS	CONDUCTIVITY $(OHM\ CM)^{-1}$	E/T MICROVOLTS/°K
77.3		4.98×10^{-3}	
78.5	.01324		37.6
80.3	.01333		37.7
81.7		4.77	
83.1	.01338		37.6
84.0		4.66	
84.6	.01341		37.5
87.0	.01355		37.6
89.5		4.37	
90.3	.01344	4.20	37.0
71.2	.01244		36.1
75.7		4.77	
77.5	.01343		38.3
81.0	.013495		38.1
83.3		4.70	
83.7	.01359		38.1
85.4	.01364		38.1
87.0	.01371		38.1
87.6		4.47	
89.2	.01389		38.3
90.8	.01420		39.0
91.9		4.40	
92.3	.01417		38.8
93.7		3.90	
95.5	.01405		38.1
96.7		3.81	

TABLE 6 - CELL NO. 51

TEMPERATURE °C	EMF, VOLTS	CONDUCTIVITY $(OHM\ CM)^{-1}$	E/T MICROVOLTS/°K
98.4	.01401		37.7
100		3.60×10^{-3}	
99.8	.01416		38.0
110.8	.01483		38.6
89.1	.01476		40.7
89.1		3.85	
90.5	.01468		43.0
92.3		3.90	
92.3	.01470		42.2
97.5	.01471		39.7
99.0		3.62	
100.5	.01469		39.3
104.0		3.40	
106.1	.01482		39.1
108.5		3.11	
110.5	.01514		39.5
112.8		2.86	
114.7	.01550		40.0
115.0	.01578		40.7
117.4		2.38	
118.0	.01619		41.4
118.4		2.10	
117.8	.01628		41.6
119.2		1.91	
122.4	.01544		39.0
124.0		1.68	

TABLE 6 - CELL NO. 51

TEMPERATURE ^{o}C	EMF, VOLTS	CONDUCTIVITY, $(OHM\ CM)^{-1}$	E/T, MICROVOLTS/^{o}K
128.0	.01640		40.9
129.9		1.65×10^{-3}	
130.0	.01650		40.9
132.0		1.58	
133.8	.01727		42.4
133.8		1.55	
136.0	.01775		43.4

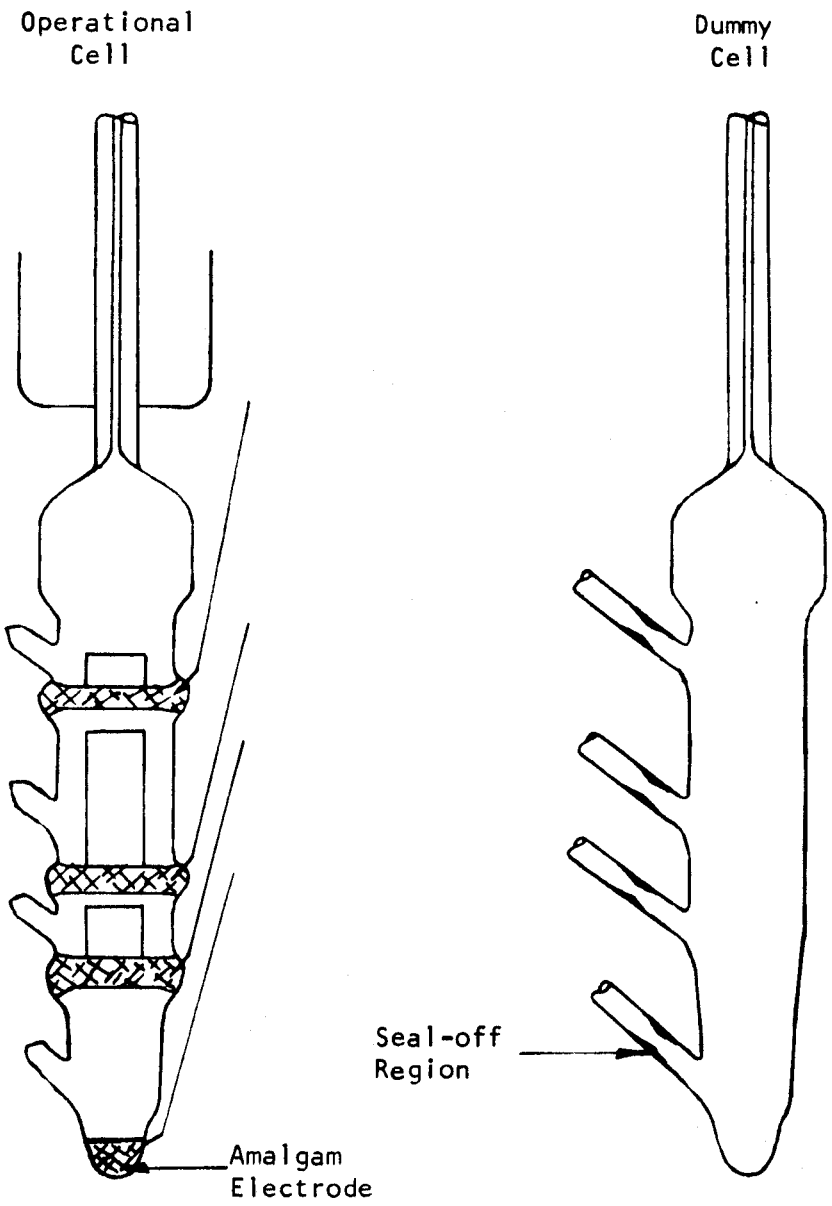

Figure 1. Cell used with insoluble salts

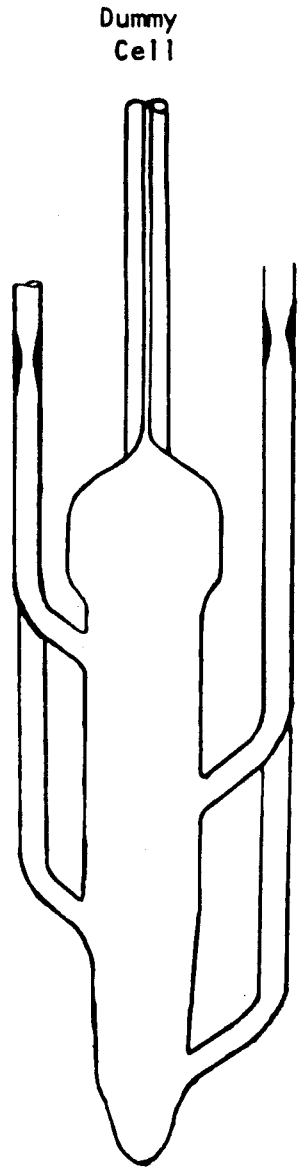

Figure 2. Cell with seal-offs remote from the neighborhoods of the amalgam electrodes.

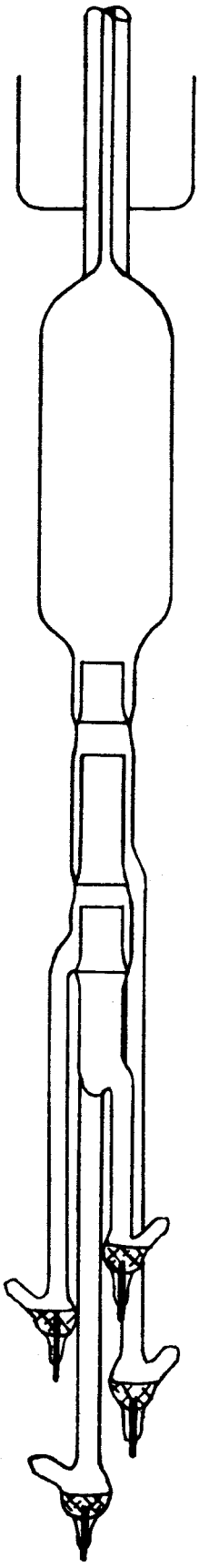

Figure 3. Cell with seal-off region relocated for maximum access during seal-off

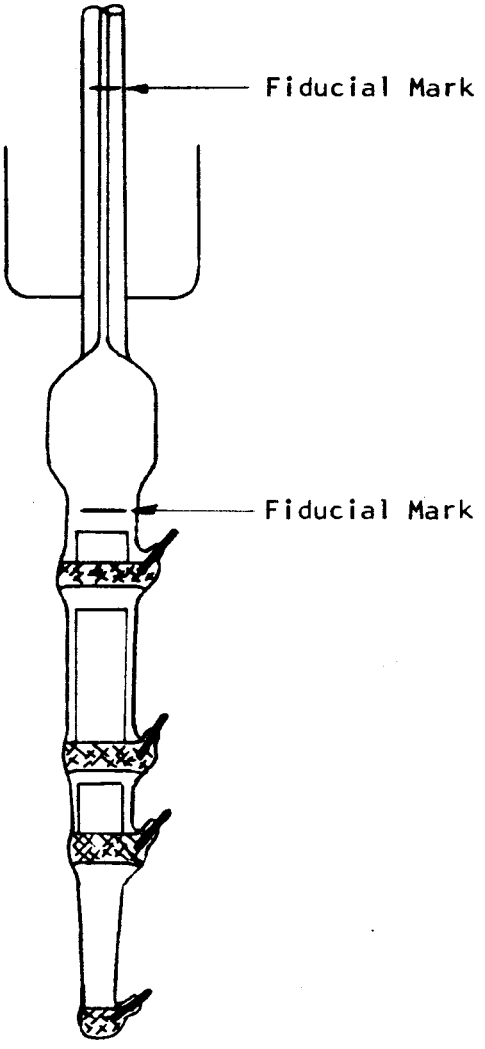

Figure 4. Present cells, without side arms, with fiducial marks for establishing volumes

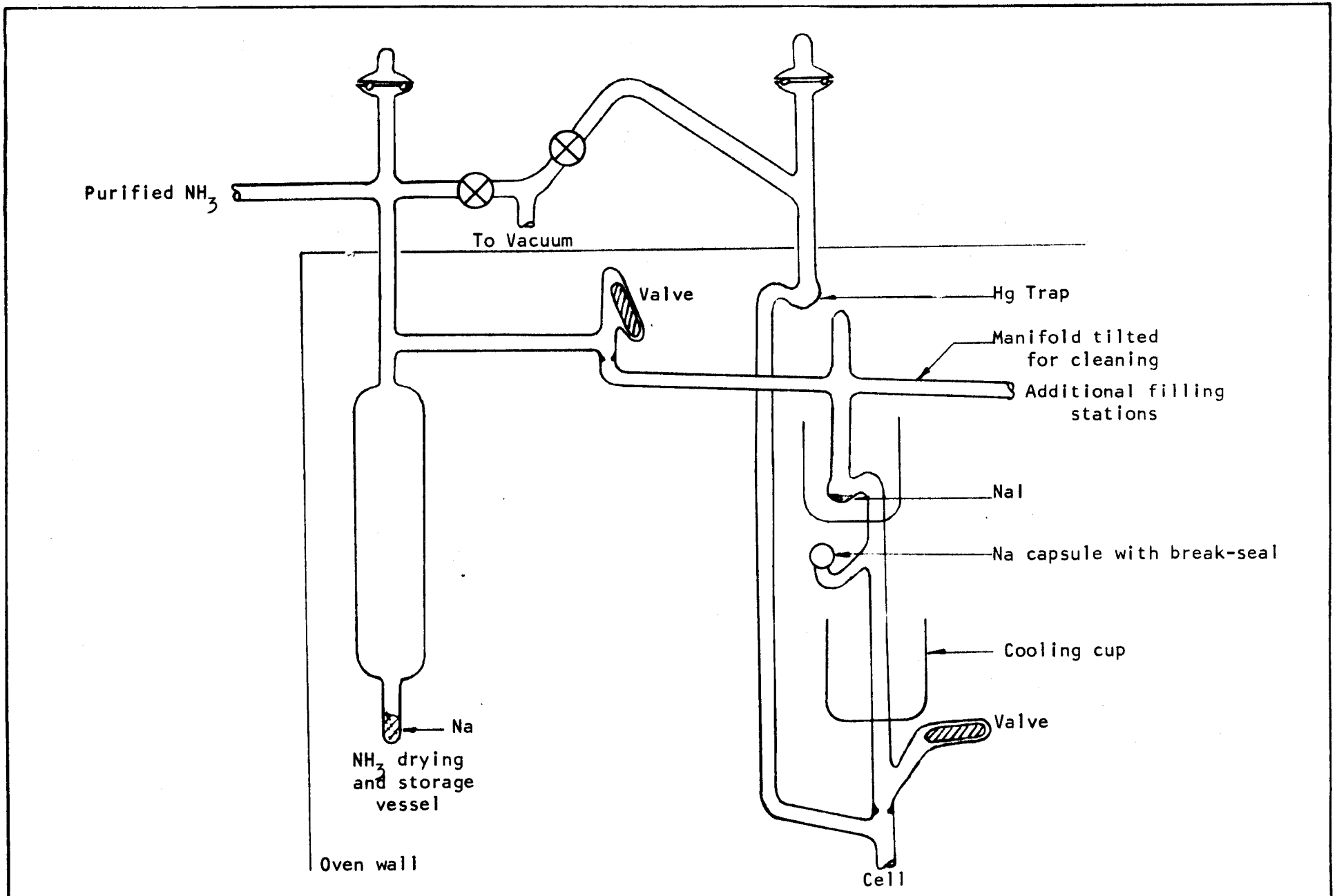

Figure 5. Bakeable vacuum system for filling electrochemical cells.

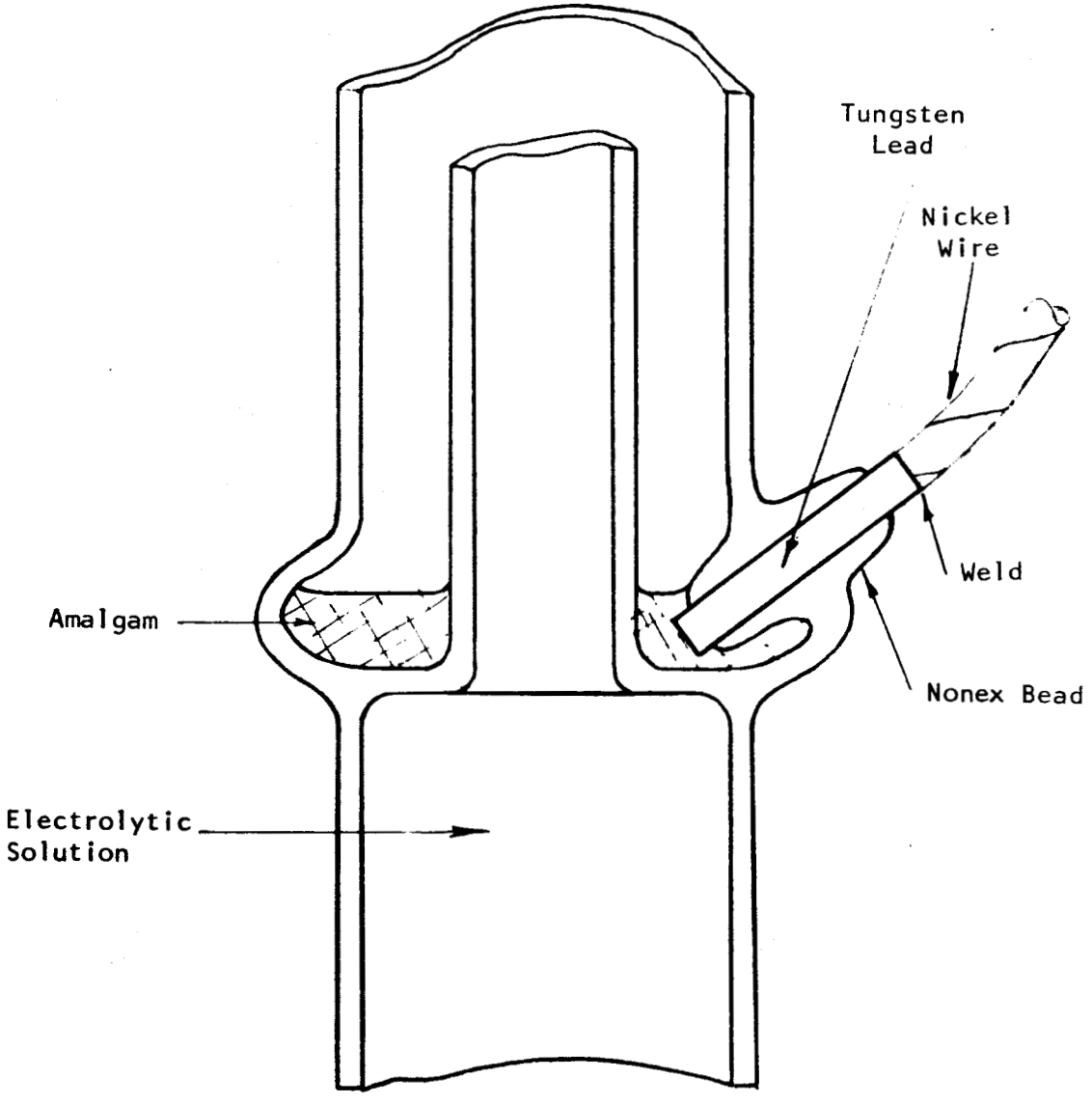

Figure 6. Cell Electrode - Cross Section

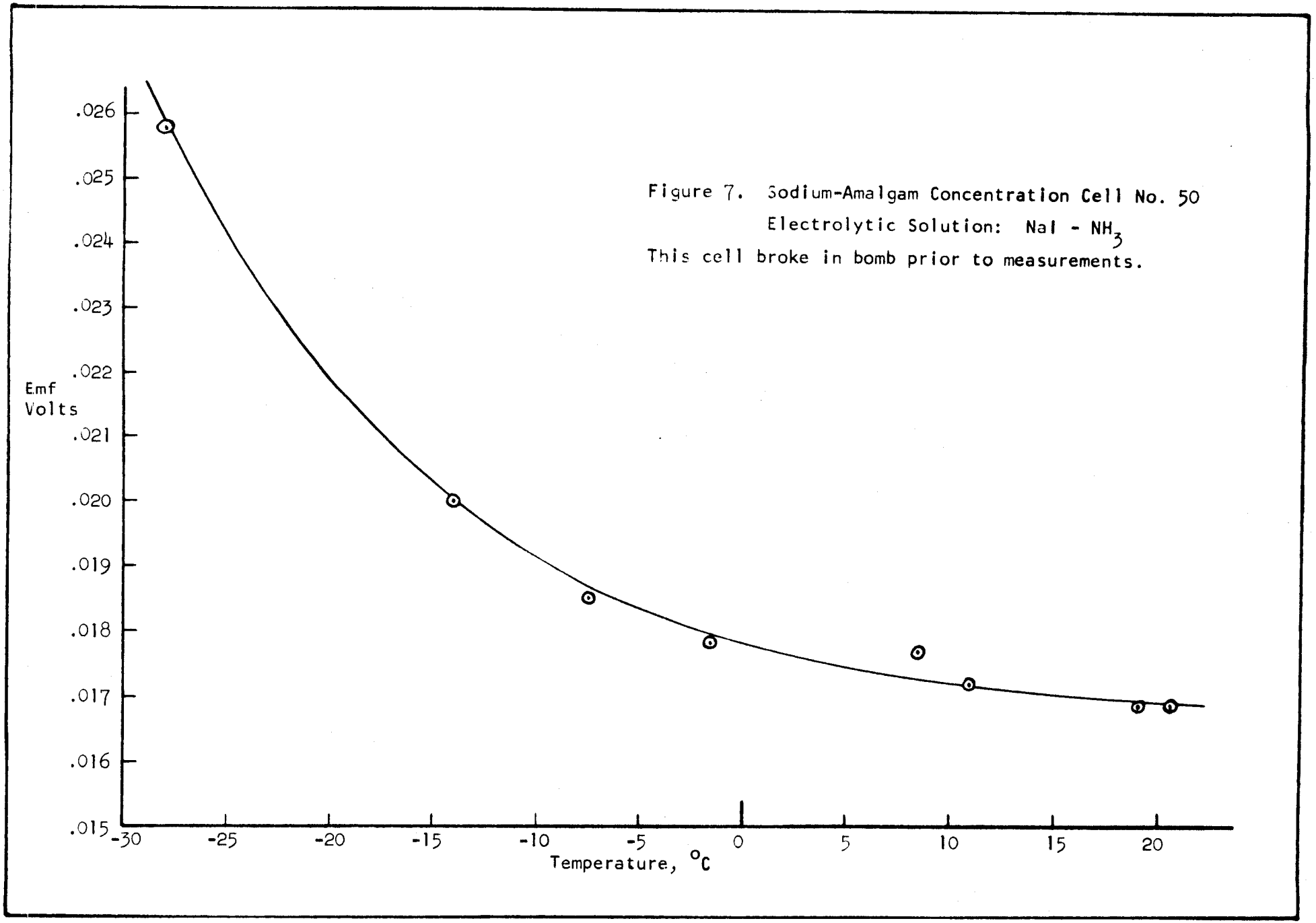

Figure 7. Sodium-Amalgam Concentration Cell No. 50

Electrolytic Solution: NaI - NH_3

This cell broke in bomb prior to measurements.

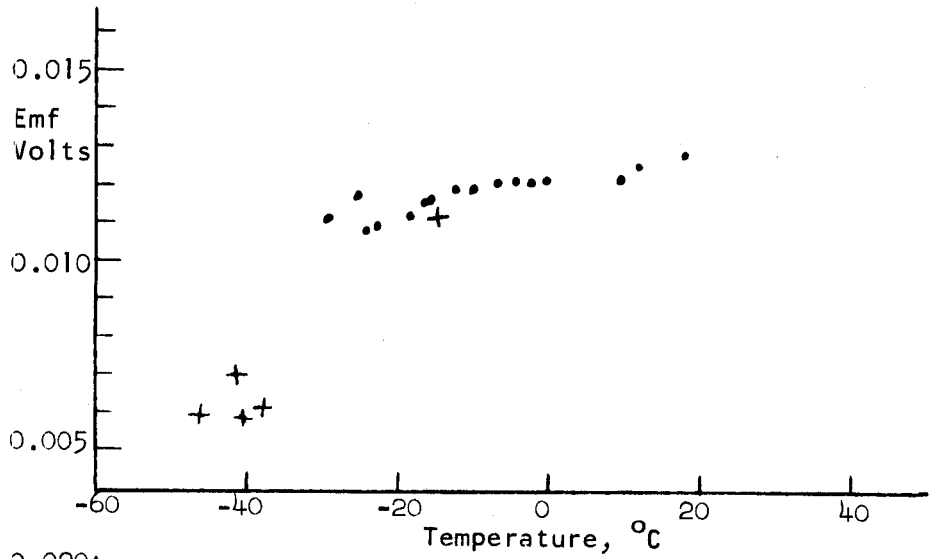

Sodium-Amalgam Concentration Cell No. 51
Electrolytic Solution: $NaI-NH_3$

Figure 8 (Opposite). These measurements were made before any current was passed through the cell.

Figure 9 (Below). These measurements were alternated with conductivity measurements, when current was passed through the cell using the working electrodes.

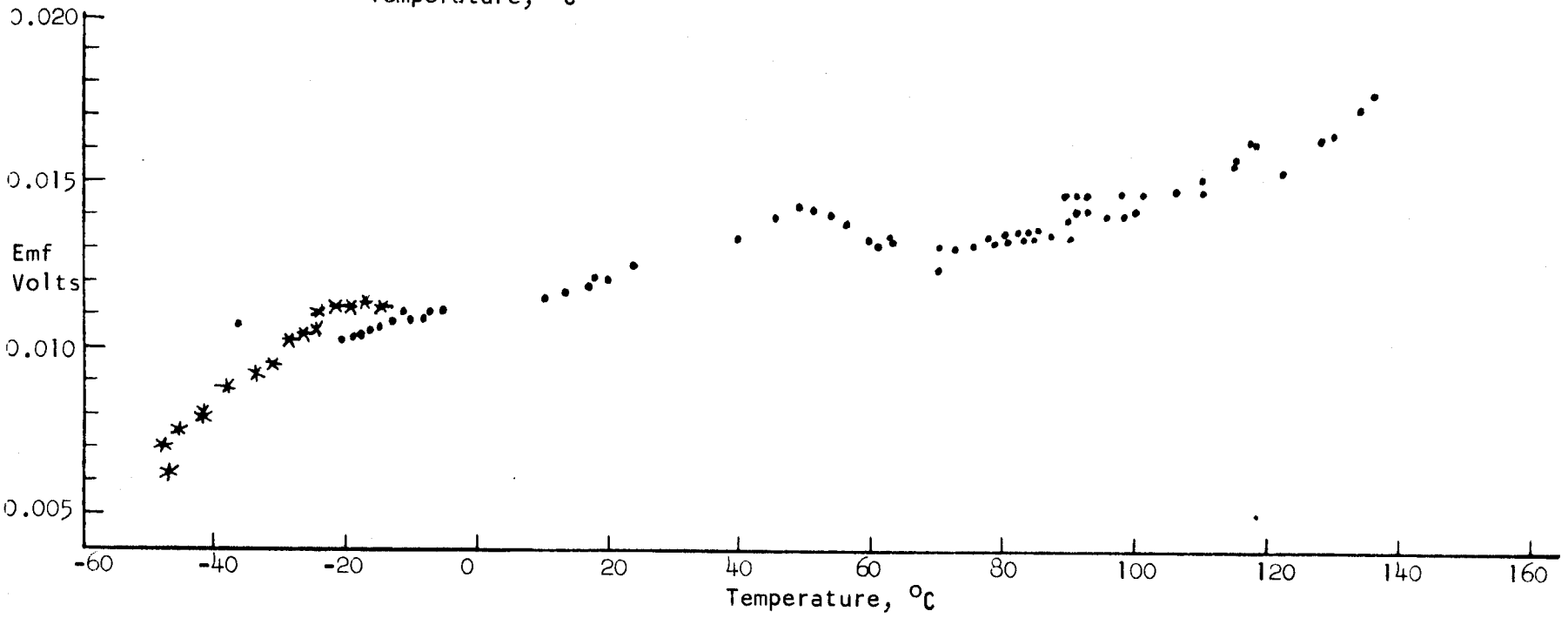

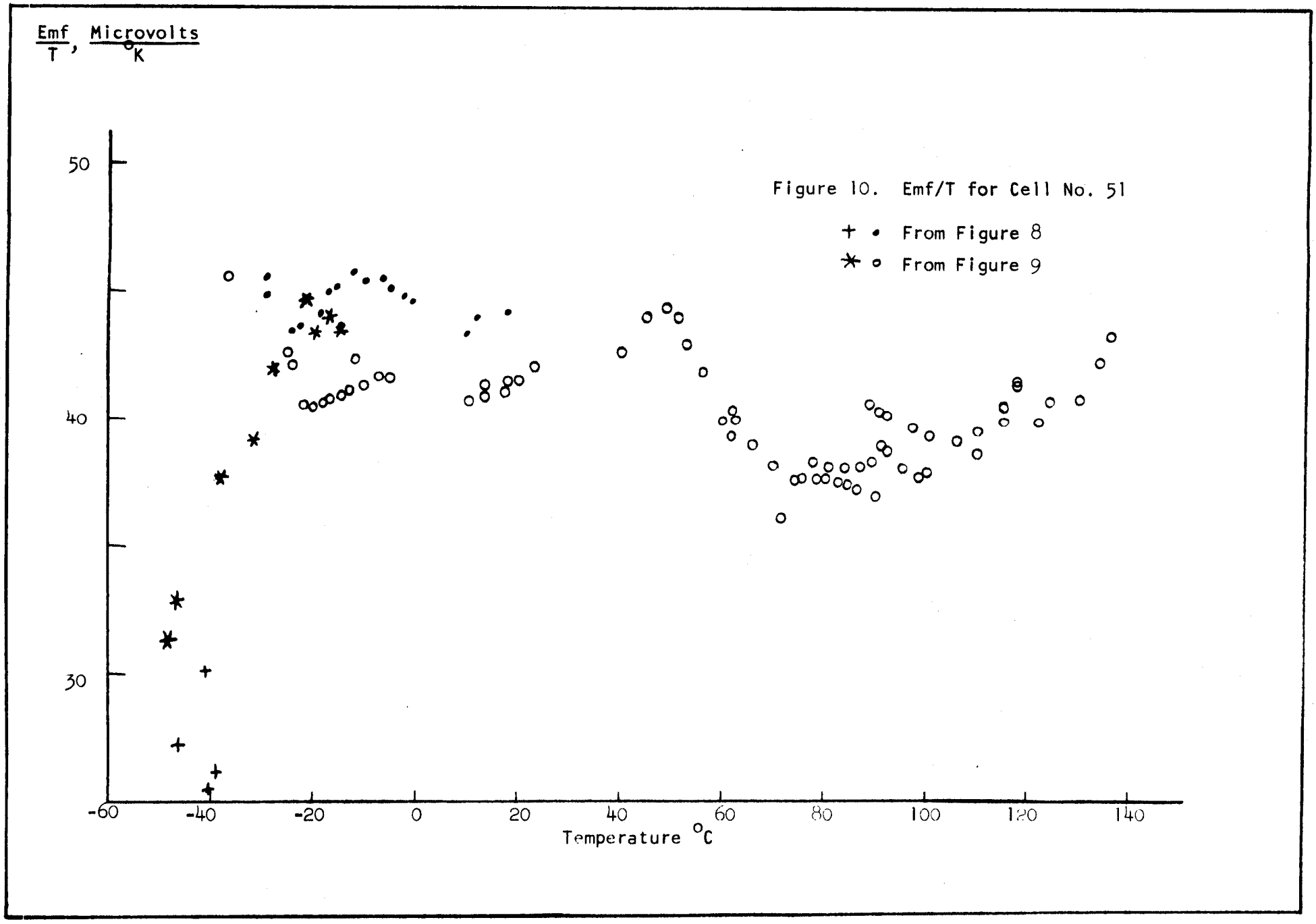

Figure 10. Emf/T for Cell No. 51

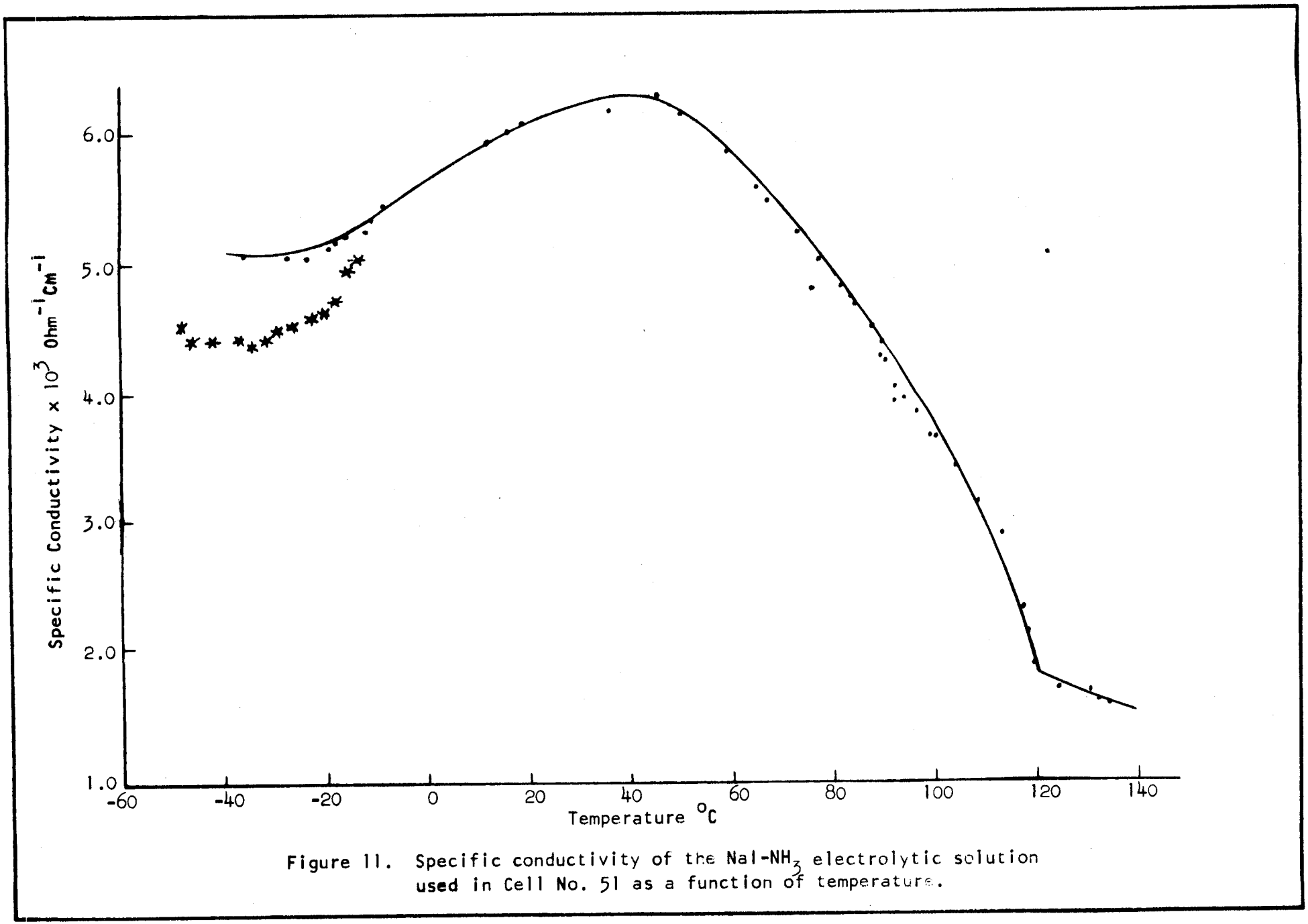

Figure 11. Specific conductivity of the $NaI-NH_3$ electrolytic solution used in Cell No. 51 as a function of temperature.

DISTRIBUTION LIST

National Aeronautics and Space Administration (6)
Washington, D.C. 20546
Attn: Ernst M. Cohn, Code RNW
James R. Miles, Code SL
A. M. Andrus, Code ST

National Aeronautics and Space Administration
Scientific and Technical Information Facility
P. O. Box 5700
Bethesda, Maryland, 20014 (3)

National Aeronautics and Space Administration
Ames Research Center
Moffett Field, California
Attn: A. S. Hertzog/J. R. Swain

National Aeronautics and Space Administration
Goddard Space Flight Center
Greenbelt, Maryland
Attn: Thomas Hennigan, Code 636
Joseph Sherfey, Code 652

National Aeronautics and Space Administration
Langley Research Center
Langley Station
Hampton, Virginia
Attn: S. T. Peterson/Harry Ricker

National Aeronautics and Space Administration
Lewis Research Center
21000 Brookpark Road
Cleveland, 35, Ohio
Attn: Irving Warshawsky
Robert Miller
N. D. Sanders
Robert L. Cummings

National Aeronautics and Space Administration
Marshall Space Flight Center
Huntsville, Alabama
Attn: Philip Youngblood

National Aeronautics and Space Administration
Manned Spacecraft Center
Houston, 1, Texas
Attn: Richard Ferguson (for EP-5)
Robert Cohen
James T. Kennedy
Forrest E. Eastman, EE-4

NASA-Western Operations Office
150 Pico Boulevard
Santa Monica, California 90406
Attn: Contract Specialist, W. A. Hall

Jet Propulsion Laboratory
4800 Oak Grove Drive
Pasadena, California
Attn: Aiji Uchiyama

DEPARTMENT OF THE ARMY

U. S. Army Engineer R and D Labs
Fort Belvoir, Virginia
Attn: Electrical Power Branch

U. S. Army Engineer R and D Labs
Fort Monmouth, New Jersey
Attn: Arthur F. Daniel (Code SELRA/SL-PS)

Harry Diamond Labs
Room 300, Building 92
Connecticut Avenue and Van Ness Street, N.W.
Washington, D.C.
Attn: Nathan Kaplan

Army Materiel Command
Research Division
AMCRD-RSCM T-7
Washington, 25, D.C.
Attn: John W. Crellin

Natick Labs
Clothing and Organic Materials Division
Natick, Massachusetts
Attn: Leo A. Spano/Robert N. Walsh

U. S. Army TRECOM
Physical Sciences Group
Fort Eustis, Virginia
Attn: (SMOFE)

U. S. Army Research Office
Box CM, Duke Station
Durham, North Carolina
Attn: Paul Greer/Dr. Wilhelm Jorgensen

U. S. Army Mobility Command
Research Division
Center Line, Michigan
Attn: O. Renius (AMSMO-RR)

Hq., U. S. Army Materiel Command
Development Division
Washington 25, D. C.
Attn: Marshall D. Aiken (AMCRD-DE-MO-P)

DEPARTMENT OF THE NAVY

Office of Naval Research
Department of the Navy
Washington 25, D. C.
Attn: Dr. Ralph Roberts/H. W. Fox

Bureau of Naval Weapons
Department of the Navy
Washington 25, D. C.
Attn: (Code RAAE)

Naval Ammunition Depot
Crane, Indiana
Attn: E.Bruess/H. Shultz

Bureau of Ships
Deparmment of the Navy
Washington 25, D. C.
Attn: Bernard B. Rosenbaum (Code 340)/C. F. Viglotti (Code 660)

Naval Ordnance Laboratory
Department of the Navy
Corona, California
Attn: Mr. William C. Spindler (Code 441)

U. S. Naval Research Laboratory
Washington, D. C., 20390
Attn: Code 6160

Naval Ordnance Laboratory
Department of the Navy
Silver Spring, Maryland
Attn: Philip B. Cole (Code WB)

DEPARTMENT OF THE AIR FORCE

Wright-Patterson AFB
Aeronautical Systems Division
Dayton, Ohio
Attn: James Elsworth Cooper

AF Cambridge Lab
L. G. Hanscom Field
Bedford, Massachusetts
Attn: Francis X. Doherty/Edward Raskind

Rome Air Development Center, ESD
Griffiss AFB, New York
Attn: Frank J. Mollura

Capt. William Hoover
Air Force Ballistic Missile Division
Attn: WEZYA-21
Air Force Unit Post Office
Los Angeles, 45, California

Space Systems Division
Los Angeles AF Station
Los Angeles, California 90045
Attn: SSSD

ATOMIC ENERGY COMMISSION

Mr. Donald B. Hoatson
Army Reactors, DRD
U. S. Atomic Energy Commission
Washington, 25, D.C.

OTHER GOVERNMENT AGENCIES

Defense Documentation Center Headquarters
Cameron Station, Bldg. 5
5010 Duke Street
Alexandria, 4, Virginia

Institute for Defense Analyses
400 Army-Navy Drive
Arlington, Virginia 22202
Attn: Dr. G. Szego/Mr. R. Hamilton

National Bureau of Standards
Washington, 25, D.C.
Attn: Dr. W. J. Hamer

Power Information Center
University of Pennsylvania
Moore School Building
200 South 33rd Street
Philadelphia, 4, Pennsylvania

Office of Technical Services
Department of Commerce
Washington, D.C. 20009

Mr. R. A. Eades
D. R. S.
British Embassy
3100 Massachusetts Avenue, N.W.
Washington, 8, D. C.

Canadian Joint Staff
Defense Research Member (NASA)
2450 Massachusetts Avenue, N.W.
Washington, 25, D.C.

PRIVATE INDUSTRY

Aerospace Corporation
P. O. Box 95085
Los Angeles, 45, California
Attn: Library

Bell Laboratories
Murray Hill, New Jersey
Attn: U. B. Thomas/David A. Feder

Boeing Airplane Company
Seattle, Washington
Attn: Henry Oman

Borden Chemical Co.
Central Research Laboratory
P. O. Box 9524
Philadelphia 24, Pennsylvania
Attn: Dr. H. L. Pfluger

Burgess Battery Company
Freeport, Illinois
Attn: Dr. Howard J. Strauss

C and D Batteries
Division of Electric Autolite Company
Conshohocken, Pennsylvania
Attn: Dr. Eugene Willihnganz

Calvin College
Grand Rapids, Michigan
Attn: Prof. T. P. Dirkse

Delco Remy Division
General Motors Corporation
Anderson, Indiana
Attn: Dr. J. J. Lander

Eagle-Picher Company
Post Office Box 290
Joplin, Missouri
Attn: E. M. Morse

Electric Storage Battery Company
Missile Battery Division
Raleigh, North Carolina
Attn: A. Chreitzberg

Electric Storage Battery Company
Carl F. Norberg Research Center
Yardley, Pennsylvania
Attn: Dr. R. A. Schaefer

Electrochimica Corporation
1140 O'Brien Drive
Menlo Park, California
Attn: Dr. Morris Eisenberg

Engelhard Industries, Inc.
497 DeLancy Street
Newark 5, New Jersey
Attn: Dr. J. G. Cohn

Dr. Arthur Fleischer
466 South Center Street
Orange, New Jersey

General Electric Company
Battery Products Section
P. O. Box 114
Gainesville, Florida

General Electric Corporation
Schenectady, New York
Attn: Dr. William Carson, ATL

General Electric Company
Missile and Space Division
Spacecraft Department
P. O. Box 8555
Philadelphia 1, Pennsylvania
Attn: E. W. Kipp, Room T-2513

General Motors Corporation
Box T
Santa Barbara, California
Attn: Dr. C. R. Russell

Globe Union Inc.
900 East Keefe Avenue
Milwaukee, Wisconsin
Attn: Dr. C. K. Morehouse

Gould-National Batteries, Inc.
Engineering and Research Center
2630 University Avenue, S.E.
Minneapolis, 14, Minnesota
Attn: J. F. Donahue

Gulton Industries
Alkaline Battery Division
Metuchen, New Jersey
Attn: Dr. Robert Shair

Inland Testing Laboratories
Dayton, Ohio
Attn: W. Ingling

Mr. B. S. Baker
Institute of Gas Technology
State and 34th Streets
Chicago, 16, Illinois

Johns Hopkins University
Applied Physics Laboratory
8621 Georgia Avenue
Silver Spring, Maryland
Attn: Richard Cole

Hughes Aircraft Corporation
Power Systems and Test Operations Dept.
El Segundo, California
Attn: R. B. Robinson

Leesona Moos Laboratories
Lake Success Park, Community Drive
Great Neck, New York 11021
Attn: Dr. H. Oswin

Arthur D. Little, Inc.
Acorn Park
Cambridge, Massachusetts 02140
Attn: Dr. Ellery W. Stone

Livingston Electronic Corporation
Route 309, Opposite Springhouse Quarry
Montgomeryville, Pennsylvania
Attn: William F. Meyers

Lockheed Aircraft Corporation
1123 N. Mathilda Avenue
Sunnyvale, California
Attn: Charles Burell

Lockheed Missiles and Space Company
Sunnyvale, California
Attn: Dr. J. E. Chilton, Dept. 52-30/
Larry E. Nelson, Dept. 65-82

P. R. Mallory and Company
Technical Services Laboratories
Indianapolis 6, Indiana
Attn: A. S. Doty

P. R. Mallory and Company
Northwest Industrial Park
Burlington, Massachusetts
Attn: Dr. Per Bro

Monsanto Research Corporation
Evertte 49, Massachusetts
Attn: Dr. J. O. Smith

North American Aviation
12214 Lakewood Blvd.
Downey, California
Attn: Burton M. Otzinger

Dr. John Owen
P. O. Box 87
Bloomfield, New Jersey

Radiation Applications Incorporated
36-40 37th Street
Long Island City 1, New York
Attn: Munroe F. Pofcher

Radio Corporation of America
Astro Division
Heightstown, New Jersey
Attn: Seymour Winkler

Radio Corporation of America
P. O. Box 800 Princeton, New Jersey
Attn: Paul Wiener

Radio Corporation of America
Somerville, New Jersey
Attn: Semiconductor and Materials Division

Sonotone Corporation
Saw Mill River Road
Elmsford, New York
Attn: A. Mundel

Space Technology Laboratories, Inc.
2400 E. El Segundo Boulevard
El Segundo, California
Attn: Dr. A. Krausz

Power Sources Division
Telecomputing Corporation
Denver, Colorado
Attn: Borch Winder

Union Carbide Corporation
PARMA Research Center
Box 6116
Cleveland, 1, Ohio
Attn: Meredith Wright

University of California
Chemistry Department
Berkeley, California
Attn: Dr. C. Tobias

University of Pennsylvania
Electrochemistry Laboratory
Philadelphia, 4, Pennsylvania
Attn: Prof. J. O'M. Brockris

Yardney Electric Corporation
40-50 Leonard Street
New York, 13, New York
Attn: Dr. Paul Howard

Power Sources Division
Whittaker Corporation
P. O. Box 337
Newbury Park, California
Attn: John Rhyne